IOP Publishing Journal of Physics B: Atomic, Molecular and Optical Physics

J. Phys. B: At. Mol. Opt. Phys. **40** (2007) 3693–3705 doi:10.1088/0953-4075/40/18/009

Controlling atom motion through the dipole–dipole force

M L Wall[1], **F Robicheaux**[1] **and R R Jones**[2]

[1] Department of Physics, Auburn University, AL 36849-5311, USA
[2] Department of Physics, University of Virginia, Charlottesville, VA 22904-0714, USA

Received 30 May 2007, in final form 20 July 2007
Published 7 September 2007
Online at stacks.iop.org/JPhysB/40/3693

Abstract

We describe simulations that illustrate the possibility for manipulating the position correlation of atoms in a magneto-optical trap (MOT) using the dipole–dipole interaction. The control scheme utilizes a narrow band laser that is detuned to the high-frequency side of a single-photon Rydberg transition in an isolated atom. As two atoms move near each other, they can be laser excited to repelling diatomic Rydberg–Rydberg potential energy curves which halt their approach. By chirping the laser from large to small detunings, atoms in a MOT can be pushed apart by dipole–dipole forces, thereby controlling nearest-neighbor interactions. Alternatively, by holding the frequency of the Rydberg excitation laser fixed as the MOT is loaded, it should be possible to limit the minimum distance between atoms to a prescribed value.

1. Introduction

Isolated Rydberg atoms are extremely sensitive to externally applied electric fields. Accordingly, when two or more atoms are in close proximity, each may be strongly influenced by the dipole field of the other(s) via resonant and/or non-resonant dipole–dipole interactions. Spectroscopically, if the Rydberg atom density is sufficiently high, the frequencies associated with allowed transitions measurably shift and broaden [1–3]. Also, transitions that are forbidden within isolated atoms may become allowed in the presence of other Rydberg atoms [2, 4]. There is considerable current interest in the processes that govern the behavior of Rydberg gases in the regime where the atom–atom interaction strength becomes comparable to other energy scales in the problem. These effects include the dipole blockade [5–14], the hopping of Rydberg excitation through an ensemble [15–21], and long-range collisions between pairs of Rydberg atoms [22–28]. Controlling these phenomena is critical for their application in areas such as quantum information processing [5, 6] or for utilizing Rydberg atoms to simulate quantum many-body models. Since the dipole–dipole interaction strength drops off rapidly (R^{-3} and R^{-6} for the resonant and non-resonant cases, respectively) with

0953-4075/07/183693+13$30.00

increasing distance R between atoms, the ability to manipulate nearest-neighbor separations is the key to controlling the atomic interactions.

More generally, techniques to create ordered arrays of neutral atoms at arbitrary separation or ensembles of atoms with well-defined minimum separation would be beneficial for a variety of applications. In principle, localizing atoms at a separation R is possible using either a periodic array of externally generated trapping potentials, e.g. an optical lattice, or by confining atoms with strong repulsive interactions within a global trapping potential. The latter case is analogous to the situation in a crystalline solid or to ion crystallization in a Penning or Paul trap [29, 30]. In either case, the atoms will have well-defined separations provided that the change in the potential energy over distances $\ll R$ exceeds $k_B T$. Fortunately, using standard laser cooling and trapping techniques one can readily produce ensembles of atoms with extremely low temperatures, T. Unfortunately, while generating an optical lattice is straightforward, achieving a unit filling fraction with only one atom per lattice site is quite challenging [31]. Also, due to the short range of the interatomic forces, observing the effect of repulsive interactions on the density or position correlation of trapped ground-state or weakly-excited neutral atoms would be extremely difficult. Instead, we describe a method that exploits long-range repulsive Rydberg–Rydberg interactions to restrict the distance of closest approach between atoms in a MOT and to potentially produce ordered arrays of atoms without an optical lattice. The technique relies on continuous laser cooling of ground-state atoms in the MOT. Atoms may be pumped into Rydberg states depending on their relative separations, but typically remain excited for only a small fraction of their spontaneous emission lifetime.

Before describing the control scheme in detail we note that the R-dependent electronic dipole–dipole interaction energy is the origin of the mechanical force between the Rydberg atoms. In the absence of external fields, the gain(loss) of electronic energy comes from the loss(gain) of energy from the center-of-mass motion of the atoms. Provided the atoms are sufficiently cold, the electronic energy curves are followed adiabatically and correspond to effective potential curves for the atomic motion [32–37]. Attractive potential curves can support bound 'vibrational' states of the interatomic motion. Moreover, electronic excitation of nearby atoms to attractive or repulsive curves can lead to a substantial increase in the atomic kinetic energy as the atoms are accelerated toward or away from each other.

This effect can be exploited to control atomic scattering between atoms in low-lying excited states [38–41] and when they are in Rydberg states [42, 43]. By detuning the frequency of an excitation laser slightly to the red (i.e. lower frequency) of a transition in an isolated atom, pairs of atoms atoms at particular separations can be promoted to an attractive molecular potential curve. The laser detuning determines the separation between the atoms at the instant of excitation as well as the kinetic energy of the two atoms at their point of closest approach. This selective excitation can result in more rapid and energetic collisions than would otherwise occur, and therefore, can also alter the evolution of a Rydberg gas, perhaps resulting in plasma formation.

Here we propose to exploit the situation that develops when a narrow-band cw laser is detuned by an amount Δ to the blue (i.e. higher frequency) of a Rydberg transition in an isolated atom. This situation was investigated for low-lying excited states [38]. If two atoms are very far apart, their dipole–dipole potential energy is negligible, and there will only be virtual transitions to the Rydberg state. However, for nearby atoms, the interaction shifts the resonant transition frequency. In particular, there is a distance where the two-photon transition is in resonance. Imagine two ground-state atoms that are far apart. As they come together due to random motion, they hardly feel a force until they reach a distance where both atoms make a transition to a Rydberg state. Because the laser is blue detuned, the potential curve for the Rydberg–Rydberg state must be repelling. Thus, the atoms experience a strong force pushing

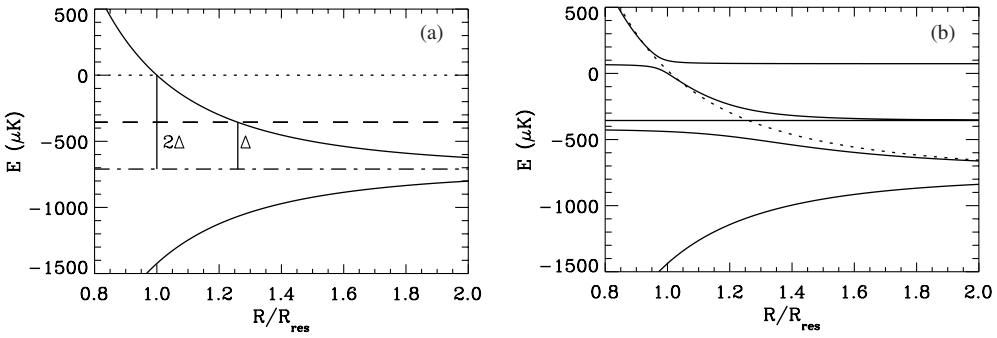

Figure 1. The Floquet energy curves for a model two-atom system with the laser detuned to the blue: (a) laser intensity is 0 and (b) laser intensity gives a single-atom Rabi frequency of 2.5 MHz. In (a), the solid lines are the Rydberg–Rydberg states, the dashed lines are the two states with one atom in the Rydberg state and the other in the ground state, and the dotted line is for both atoms in the ground state. The distance has been scaled to the separation $R_{\rm res}$ where the repelling Rydberg–Rydberg state is in resonance. The dash-dot line shows the position of the Rydberg–Rydberg state if the interaction between atoms is set to 0. In (b), an approximate, diabatic curve for the repelling Rydberg–Rydberg state is shown as a dotted line.

them apart. Later, as the atoms move to larger separation, they will once again go through the distance where the laser is resonant with the two-photon transition. The atoms then emit photons and end up in the ground state. As discussed in more detail below, the two-photon absorption and emission is accomplished via adiabatic rapid passage between dressed states. This process can occur with arbitrarily high efficiency, provided there is sufficient laser power for a given relative velocity between atoms, supplying a controllable interatomic force that acts to keep the atoms separated while only having the atoms in the Rydberg state for a short time.

To see how this situation develops, examine the Floquet energy levels in figure 1 for a model of two atoms interacting with a laser field and each other. Details of the model are given in the next section. In figure 1(a), we show the Floquet energy levels with the laser strength set to 0. For this model, we assume the Rydberg–Rydberg interaction occurs through a dipole–dipole potential that couples a pair of (nearly) degenerate states of opposite parity. There are many, many possible examples of this scenario including the Rb $48s_{1/2}48s_{1/2}$ + $47p_{3/2}48p_{3/2}$ states from [43] or the Cs $23p_{3/2}23p_{3/2} + 23s_{1/2}24s_{1/2}$ levels from [16]. The two Rydberg states become mixed and have energies of $2E_{\rm Ryd} \pm C/R^3$. In figure 1(a), the two solid lines are the Floquet energies for the two eigenstates in the presence of the dipole–dipole interaction. The dashed line in figure 1(a) shows the two states with one atom in the Rydberg state and the other in the ground state (degenerate levels) and the dotted line is for both atoms in the ground state. We will use the symbol $R_{\rm res}$ for the separation where the two-photon resonance condition is satisfied. The atomic separation length scale has been chosen so that the two-photon resonance condition occurs at 1.

Note that the repelling potential curve crosses the singly excited state at the separation $2^{1/3}R_{\rm res}$. The one-photon resonance (i.e. the one-photon transition when one of the atoms is already in a Rydberg state) is detuned by Δ but the two-photon resonance is detuned by 2Δ. The Floquet energy levels in the presence of the laser are shown in figure 1(b). Note that the crossings with the Rydberg–Rydberg state have now become avoided crossings. An approximate, diabatic curve for the repelling Rydberg–Rydberg state is shown as a dotted line. Our primary interest here is the uppermost curve. This is the dressed state that corresponds to both atoms in the ground state at large distances and the atoms in the strongly repelling Rydberg–Rydberg state at short distances.

As long as the atoms move slowly and spontaneous emission from the Rydberg states is negligible, the system will stay on the upper curve. This means the atoms can be kept far apart and will always end up in the ground state after each collision. The atoms will only be in the Rydberg states during the short amount of time needed to push them apart. This time can be much shorter than the Rydberg spontaneous emission lifetime. Another interesting feature is that the detuning of the laser determines the separation that gives the two-photon resonance: large detuning gives resonance at small separation and small detuning gives resonance at large separations. For typical pairs of Rydberg states with $n \approx 40$, the resonant separation is on the order of microns for laser detunings on the order of 10 MHz.

This leads to two interesting possibilities for cold gas experiments. The first is to start with a laser that has a large detuning and slowly chirp toward smaller detuning. The atoms then experience an inter-atomic potential whose repelling part moves to larger separations. This would give an effective force that pushes the atoms apart while they remain confined in a MOT. One might use this mechanism to push the atoms into something approximating an ordered array. The second is to use the inter-atomic potential to control the properties of an ultracold gas. A MOT could be loaded with a fixed frequency Rydberg laser in place. One would then have an interaction where both the scattering length and range of the potential can be controlled. Moreover, the range of the potential is enormous.

In the following sections, we give the results of calculations that illuminate the properties of the potential curves. We first describe a model that captures the essence of this physical situation. We then give two examples in Rb that demonstrate some of the complications that develop for real systems.

Atomic units are used throughout this paper unless specifically noted otherwise.

2. A model system

In this section, we consider a model system that captures the essence of the Rydberg–Rydberg interaction. We use five electronic states to characterize the two-atom system. Physically we want to represent the case where a laser is detuned slightly from a transition between a ground- or low-lying excited-state and a Rydberg state r_a. The transition does not occur for isolated atoms because the laser is too far off resonance. However, if two atoms are both in the Rydberg state r_a, they can interact through the dipole–dipole interaction. In particular, we consider the case where there is a second, (nearly) degenerate pair of states, r_b and r_b' which differ in angular momentum from r_a by ± 1. In order to simplify the calculation, we ignore the dependence of this interaction on the direction between atoms. We also assume the two pairs of Rydberg states are exactly degenerate; in practice this is easily accomplished by applying a small, static electric field to the atoms, e.g. see [15, 16, 23].

The laser–atom interaction is through a coupling term $E D_{g,r_a} \cos(\omega t)$ with D_{g,r_a} the dipole matrix element between the 'ground' state and the Rydberg state r_a and ω is the laser frequency. To put the frequency into a more useful form, we write $\omega = E_r + \Delta$ where E_r is the energy of the Rydberg state above the ground state and Δ is the detuning.

We define zero energy to be the energy where both atoms are in the electronic ground state. The five states correspond to both atoms in the ground state, $|1\rangle \equiv |gg\rangle$, atom 1 in the Rydberg state r_a and atom 2 in the ground state, $|2\rangle \equiv |r_a g\rangle \exp[-\mathrm{i}(E_r + \Delta)t]$, atom 1 in the ground state and atom 2 in the Rydberg state r_a, $|3\rangle \equiv |g r_a\rangle \exp[-\mathrm{i}(E_r + \Delta)t]$, both atoms in the Rydberg state r_a, $|4\rangle \equiv |r_a r_a\rangle \exp[-2\mathrm{i}(E_r + \Delta)t]$, and both Rydberg atoms in the opposite parity Rydberg state, $|5\rangle \equiv |r_b r_b'\rangle \exp[-2\mathrm{i}(E_r + \Delta)t]$.

When we use the rotating wave approximation, we obtain a time-independent Hamiltonian whose only nonzero matrix elements are

$$\begin{aligned} H_{12} &= H_{13} = H_{24} = H_{34} \equiv \frac{\Omega}{2} \\ H_{22} &= H_{33} = -\Delta \\ H_{44} &= H_{55} = -2\Delta \qquad H_{45} = \frac{C}{R^3} \end{aligned} \tag{1}$$

and the transposed elements $H_{kk'} = H_{k'k}$. In equation (1), Ω is 2π times the Rabi frequency for the single-atom transition between the ground state and Rydberg state r_a, R is the distance between atoms, and C parameterizes the strength of the Rydberg–Rydberg interaction. For this section, we use $C = 40^4$ au which is roughly that for strong coupling of Rydberg states near $n = 40$. The system could be simplified to four-levels by using the fact that the '$-$' state, $(|2\rangle - |3\rangle)/\sqrt{2}$, is 'dark' and does not couple to any other state. The distance that gives exact two-photon resonance is $R_{\rm res} = (C/2\Delta)^{1/3}$.

In figure 1, we show the five energies of this Hamiltonian versus the distance between the atoms. The Rabi frequency is 0 in figure 1(a) and 2.5 MHz in figure 1(b), which is a reasonable number for strongly allowed Rydberg transitions. We have set the detuning to 7.4 MHz, giving a two-photon resonance at $R = 5.5$ μm. The character of the five curves in figure 1(b) can be expressed in terms of the original, uncoupled basis states or in terms of the eigenstates in figure 1(a). Many of the qualitative features in figure 1(b) are easily understood. The state that has no dependence on R corresponds to the '$-$' superposition of states where one atom is in the ground state and the other is in a Rydberg state. The energy level crossings in figure 1(a) become avoided crossings in figure 1(b) due to the laser interaction. The avoided crossing of the $(|4\rangle + |5\rangle)/\sqrt{2}$ with the singly excited state is much larger than with the ground state because the first corresponds to a one-photon transition while the second is a two-photon transition.

2.1. Classical treatment of atom motion

Before describing a fully quantum treatment of the atomic motion, we first examine the behavior when the atomic motion is approximately classical. In this case, the pair of atoms experience a mutual force that depends on which of the electronic states the pair is in. If the atoms have a temperature of several 100 μK, their velocity is low enough that the system remains on the adiabatic potential curves. The force between the atoms can be computed from the gradient of the adiabatic energy.

The repulsive dipole–dipole force is ineffective for atoms that do not interact perfectly adiabatically. Ground-state atoms that pass diabatically through the avoided level crossing on the upper potential curve could move near each other without being excited to Rydberg states and, therefore, without any energy penalty for their approach. Worse still, there would be substantial heating of the atoms if the ground-state atoms were not continuously cooled. To see this, suppose the atoms come together on the upper potential curve and adiabatically follow it to the double Rydberg state but as they move apart the atoms make a non-adiabatic transition, either via stimulated or spontaneous emission, to the singly excited state. They would then share a kinetic energy equal to Δ. For the parameters in our model, they would each gain $\sim$180 μK worth of kinetic energy. Fortunately, however, the ground-state atoms will be rapidly cooled by the MOT trapping beams. In addition, the remaining Rydberg atom from the pair will spontaneously decay to the ground state, typically in $\sim$100 μs or less, before leaving the MOT and will also be cooled and remain trapped.

A perturbative treatment of the interactions with the singly excited states gives an approximation to the important parameters. We assume that the spontaneous lifetime of the Rydberg states has been chosen to be at least several tens of μs so that spontaneous

emission can be neglected during the few μs interval that the atoms are excited near the resonance separation. Adiabatic elimination of the single Rydberg states and the repelling double Rydberg state, results in an effective 2×2 Hamiltonian, $\tilde{H}$, with the approximate matrix elements

$$\tilde{H}_{11} = \frac{\Omega^2}{2\Delta + \Omega^2/(4\Delta - 2C/R^3)} \tag{2}$$

$\tilde{H}_{12} = \tilde{H}_{21} = (1/\sqrt{2})H_{11}$ and $\tilde{H}_{22} = (1/2)\tilde{H}_{11} + (-2\Delta + C/R^3)$. To lowest nonzero order, the $|gg\rangle$ state is AC Stark shifted by an amount $\Omega^2/2\Delta$ for large R. The repelling double Rydberg state is shifted by $\Omega^2/4\Delta$ for $R \simeq R_{\rm res}$. To lowest nonzero order, the coupling between the $|gg\rangle$ state and the two Rydberg state is $\sqrt{2}\Omega^2/(4\Delta)$.

A Landau–Zener treatment of the avoided crossing gives an approximate transition probability of the form $P = \exp\left(-2\pi \tilde{H}_{12}^2 \big/ [vd(H_{11} - H_{22})/\mathrm{d}R]\right)$. The approximate parameters from the previous paragraph allow us to estimate the transition probability in atomic units as

$$P = \exp\left[\frac{-\pi\Omega^4 R_{\rm res}^4}{12\Delta^2 C v}\right] = \exp\left[\frac{-\pi\Omega^4 (C/2)^{1/3}}{24\Delta^{10/3} v}\right] \tag{3}$$

where v is relative radial speed of the atoms and in the second step we have substituted for the resonance condition $C \big/ R_{\rm res}^3 = 2\Delta$. Note the high powers of Ω, the one-atom Rabi frequency times 2π, and Δ, the one-atom laser detuning. This means that if one can reach the region of adiabatic motion then the non-adiabatic transitions can be made almost arbitrarily small. For example, once the non-adiabatic transitions have been reduced to 10% they can be reduced to 1% by increasing Ω by a factor of 1.2. Another interesting question is how does the transition probability depend on n? The dependence is through C which is proportional to n^4; however, the exponential only depends on $C^{1/3}$ which means the transition probability is not as strongly dependent on n as might be expected.

To test whether the motion is adiabatic, we solved the time-dependent Schrödinger equation for the electronic states but used classical equations of motion for the atom positions. We fired the atoms at each other with a relative velocity of 0.84 m s^{-1} which corresponds to two Rb atoms with kinetic energy of 900 μK each. This is probably a good deal faster than atomic collisions in a MOT. We found less than 1% non-adiabatic transitions for our parameters.

2.2. The three-atom case

We propose to use this mechanism to move, and perhaps hold, atoms apart. Success will depend on whether the atoms stay on the adiabatic Floquet curves during a collision. From the previous section, it can be seen that the adiabaticity for a binary collision can be assured. We also computed the adiabaticity when three atoms collide. It is not obvious that the evolution will still be adiabatic because there can be collisions with the third atom while the other two are in Rydberg states and this might cause non-adiabatic transitions. We used the same parameters as from the previous section. However, for three atoms there are many more states in the calculation corresponding to all of the different combinations of electronic states. Again, we numerically solved the time dependent Schrödinger equation for the electronic states and allowed the atoms to move classically.

We performed two different types of calculations. First, we fired the three atoms inward on an equilateral triangle; this case guarantees that all three atoms simultaneously interact strongly with the others. Second, we confined the atoms within a small cube and let them randomly bounce into each other; we repeated this calculation for many different random

parameters for the initial positions and velocities of the atoms. There were many example cases where all three atoms strongly interacted with each other at the same time. Somewhat surprisingly, in all of the calculations, we found the level of adiabaticity to be similar to the two-atom case.

2.3. Fully quantum treatment of atom motion

In the previous sections, we treated the atomic motion of the atoms using a classical approximation. This leads to relatively straightforward calculations of the motion of the atoms using the adiabatic potential curves. We have also solved for the motion of two atoms using a fully quantum treatment of the R degree of freedom as well as the electronic states. We examined this behavior to ensure that the quantum motion did not introduce new physical processes.

In this calculation, we assume that the atoms are moving directly toward each other to guarantee the maximum motion in and out. The full wavefunction can be written as

$$|\Psi\rangle(t) = \sum_{k=1}^{5} \psi_k(R,t)|k\rangle \tag{4}$$

where the function $\psi_k(R,t)$ is proportional to the amplitude for the atoms to have electronic state k and have separation R at time t. The normalization is such that

$$1 = \int \sum_{k=1}^{5} |\psi_k(R,t)|^2 \mathrm{d}R. \tag{5}$$

The radial functions are solutions of the Schrödinger equation

$$\mathrm{i}\frac{\partial \psi_k(R,t)}{\partial t} = -\frac{1}{2\mu}\frac{\partial^2 \psi_k(R,t)}{\partial R^2} + \sum_{k'=1}^{5} H_{kk'}(R)\psi_{k'}(R,t) \tag{6}$$

with the electronic Hamiltonian $H_{kk'}$ given in equation (1). We launch incoming atomic wavepackets with radial widths $\Delta R = 250$ au $\simeq 13$ nm from an initial mean separation $R_0 = 1.15 \times R_{\mathrm{res}} \simeq 6.3$ μm at $t = 0$. The electronic part of the initial wavefunction is the adiabatic eigenstate for the upper potential curve in figure 1(b).

We find that the wave packet is reflected from the point $R = R_{\mathrm{res}}$ with more than 99% efficiency onto the adiabatic potential curve. The part of the wave that does not reflect approximately corresponds to the nonadiabatic transition calculated in the previous section. Thus, the simple picture of the atoms moving on adiabatic potential curves is confirmed by this fully quantum calculation.

3. Rb examples

We now present the results from two examples in Rb. Real atomic systems are more complicated than the model due to the large number of degenerate levels and due to the angular dependence of the interaction. The purpose of these examples is to show how these extra complications change the Floquet potential curves. In particular, the angular dependence of the interaction needs to be examined [34]. We will take the laser to be linearly polarized in the z-direction and we will investigate how the states depend on the angle between the laser and the interatomic vector. Additional complications which are not addressed here include the (small) inhomogenous magnetic field in the MOT and hyper-fine structure; these two effects are on the order of a few 10's of μK for the Rydberg states.

In both examples, we will consider excitation of the $38p_{3/2}38p_{3/2}$ Rydberg state. This state is nearly degenerate with the $38s_{1/2}39s_{1/2}$ state with an energy offset of 214 μK. In a 0.36 V cm^{-1} static electric field, all of the different magnetic sublevels of the Rydberg–Rydberg states are within 24 μK of each other. We assume that the static field is in the $+z$-direction and that negligible character of other angular momentum states is mixed into s and p-levels via the second-order Stark shift. The spontaneous lifetimes of all the bare Rydberg states are quite long, with $\tau_s \simeq 60\,\mu$s and $\tau_p \simeq 150\,\mu$s. The blackbody transitions are to nearby states and the time scale for transitions out of each of the states is approximately 50 μs for room temperature black body radiation. Also, this is a promising candidate because the radial dipole matrix element between the 38p and 38s and between the 38p and 39s are approximately equal and as big as can be expected. We computed the radial matrix element for 38p38s to be 1399 au and that for 38p39s to be 1365 au. This gives relatively strong Rydberg–Rydberg coupling for such a low n. We used the energy levels of [44] to compute these quantities. In the first case we examine, a low-lying $ns_{1/2}$ state is assumed for the ground state while in the second case we consider excitation from a $nd_{5/2}$ state. As discussed below, the sub-state structure of the ground state affects the details regarding how the atoms behave. In both cases we implicitly assume that the ground state is either directly cooled and trapped in the MOT, or laser coupled to a trapped-state with a Rabi frequency less than 1 MHz. The energy level shifts and broadening associated with the ground-state dressing, as well as the natural linewidth of the dressed ground state, are assumed to be negligible compared to the Rydberg laser detuning and the repulsive dipole–dipole splitting near $R_{\rm res}$. In addition, for the low-MOT densities we consider, laser coupling of the cycling levels in the MOT to the lower level of the Rydberg transition is expected to have little effect on the temperature and number of atoms in the MOT. When excited, the atoms are neither cooled nor subjected to the primary source of heating due to the MOT beams and collisional losses due to excited atoms should be small.

We will denote the states by $|n, \ell, j, m_j\rangle$. All of the terms in the Hamiltonian can be found from the single-atom dipole matrix elements. Using standard angular momentum recoupling, the matrix elements are found using

$$\langle n', \ell', j', m'_j|r_q^{(1)}|n, \ell, j, m_j\rangle = -1^{j'+j+3/2-m'_j}\sqrt{(2j'+1)(2j+1)(2\ell'+1)(2\ell+1)} \times \begin{pmatrix} j & j' & 1 \\ m_j & -m'_j & q \end{pmatrix} \begin{pmatrix} \ell & \ell' & 1 \\ 0 & 0 & 0 \end{pmatrix} \begin{Bmatrix} 1 & \ell & \ell' \\ \frac{1}{2} & j & j' \end{Bmatrix} \int_0^\infty R_{n'\ell'j'}(r) R_{n\ell j}(r) r\,{\rm d}r \quad (7)$$

where we use the conventions of [45]. We computed the radial matrix elements numerically by solving for the radial functions using a Numerov approximation at the observed values for the energies [44] to determine the radial functions. The matrix elements of x, y, z are determined using the relations:

$$x = \frac{r_{-1}^{(1)} - r_1^{(1)}}{\sqrt{2}} \qquad y = {\rm i}\frac{r_{-1}^{(1)} + r_1^{(1)}}{\sqrt{2}} \qquad z = r_0^{(1)}. \quad (8)$$

The laser–atom interaction can be found directly from these dipole matrix elements. The interaction between the Rydberg states requires the summation over the operators embodied in the expression

$$\underline{DD} = \vec{r}_1 \cdot \vec{r}_2 - 3(\vec{r}_1 \cdot \hat{R})(\vec{r}_2 \cdot \hat{R}) \quad (9)$$

where $\hat{R}$ is the unit vector pointing from atom 1 to 2.

3.1. Example $5s_{1/2} + \hbar\omega \rightarrow 38p_{3/2}$

In this section, we present results for when the initial state is a compact s state. All compact s states present the same qualitative behavior. We chose the initial state to be the $5s_{1/2}$

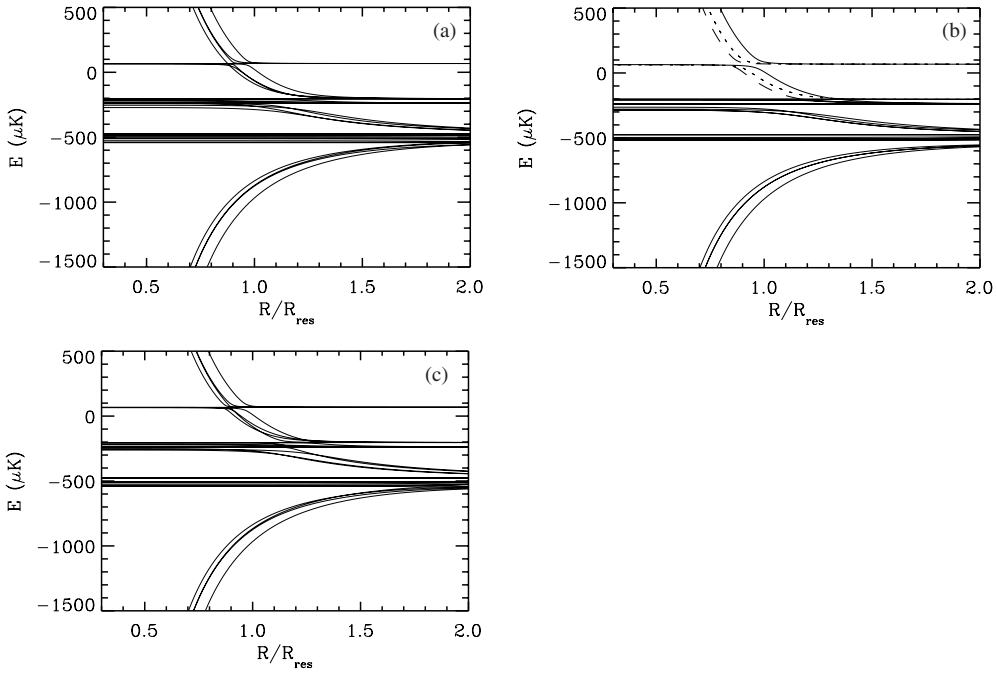

Figure 2. Same as figure 1 but for the Rb states described in section 3.1. In all of the plots, the laser detuning was 4.94 MHz $\simeq$ 237 μK. The scale length is $R_{\rm res} = 5.2$ μm. In (a)–(c) the angle between the laser and interatomic axis is 54.7°, 0° and 90°, respectively. In (b), we show the curves associated with specific avoided crossings with different line types.

state which gives a transition wavelength of ∼300 nm. We compute a radial dipole matrix element with the 38p state of 6×10^{-3} au by numerically solving for the radial functions in a model potential that gives the correct quantum defects. For the calculation, we chose the laser intensity to be 400 W cm^{-2}. Obtaining such a high intensity from a laser at this frequency within a bandwidth less than the Rydberg transition Rabi frequency (<1 MHz or so) is experimentally challenging and expensive. However, any compact s state will give the same results as long as the laser intensity is chosen to have $E \cdot D/2 \sim 100$ μK, i.e. a Rabi frequency of a few MHz.

First, we count the number of states: there are 4 states with $5s_{1/2}5s_{1/2}$ character, there are 8 states with $5s_{1/2}38p_{3/2}$ character and 8 with the order interchanged, there are 16 states with $38p_{3/2}38p_{3/2}$ character, and there are 4 states with $38s_{1/2}39s_{1/2}$ character and 4 with the order interchanged. This gives 44 states altogether.

In figure 2, we show the Floquet potential curves as a function of the atom separation for three different directions between the laser polarization and the interatomic direction. In all of the plots, the laser detuning is 4.94 MHz $\simeq$ 237 μK. We defined the scale length to be $R_{\rm res} \equiv (n^4/3\Delta)^{1/3}$ which corresponds to 5.2 μm. Unlike in the simple model, there are several Rydberg–Rydberg potential curves and thus several resonance distances.

It is clear that the Floquet curves are more complicated but the general structure of the 5-state model is preserved. In particular, the curves that have both atoms in the ground state at large distances always become strongly repelling when the atoms get inside the resonance distance. Thus, the basic mechanism will also work for this configuration. However, the sizes of the avoided crossings depend on the angle.

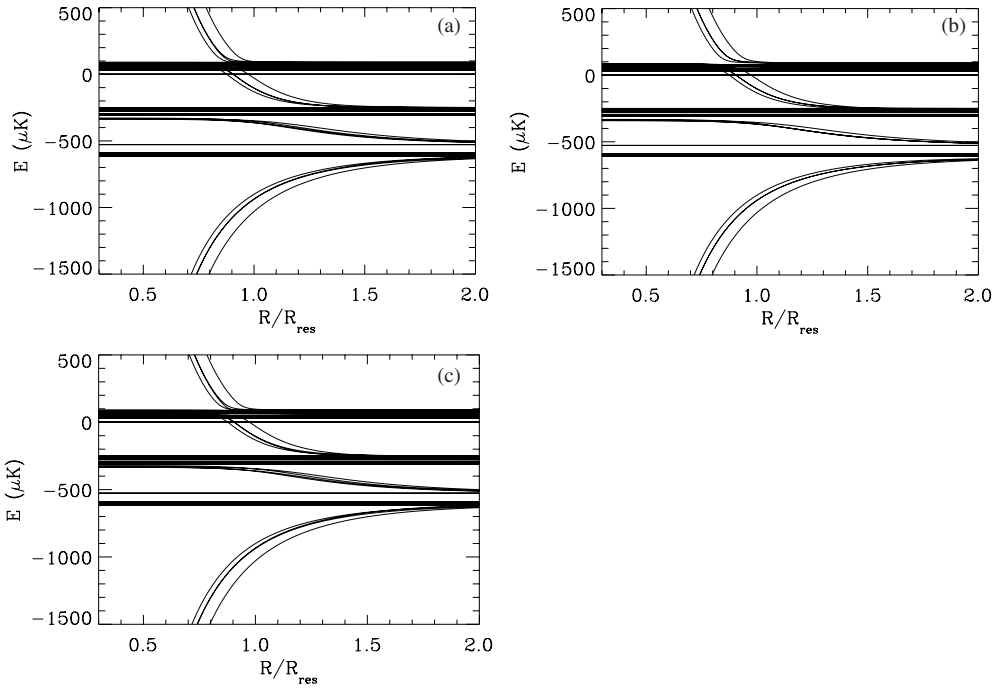

Figure 3. Same as figure 2 but for the Rb states described in section 3.2. In all of the plots, the laser detuning was 5.50 MHz $\simeq$ 264 μK. The scale length is $R_{\rm res} = 5.0$ μm.

There are a number of interesting features of the Floquet curves at a fixed angle. Of the 24 Rydberg–Rydberg states, there are 4 repelling potential curves and 4 attracting potential curves. The other 16 Rydberg–Rydberg curves have no R dependence for a fixed angle; these are the states with Föster zeros [34]. There are 16 zeros because there are 24 states with only 8 off-diagonal rows (columns) in the Rydberg–Rydberg part of the Hamiltonian. In all of the figures, it appears that there are close avoided crossings for the upper potential curves. For figures 2(b) and (c), this is an illusion; these are the cases where the angle between the laser and the interatomic axis are parallel or perpendicular. For example in figure 2(b), we have shown the curves with the avoided crossing using like line types; the two solid curves are involved in an avoided crossing, likewise for the two dashed curves and the two dotted curves but the dashed and dotted curves do not affect the other.

The situation is different for angles near $\theta = 54.7^\circ$, figure 2(a). In this case, one of the four curves has a diabatic crossing. Therefore, there is a range of angles where one of the crossings will change from diabatic to adiabatic. This circumstance would limit the applicability of the repelling force. There are two ways to circumvent this limitation. (1) Use a restricted geometry where the atoms can only approach each other with angles away from $\theta = 54.7^\circ$; for example, have the light focused down to a narrow sheet or down to a narrow cylinder [26]. (2) Use a different polarization. For example, with a combination of linear and circular polarized light, the AC Stark shifts of the four ground states are nondegenerate and the highest Stark shift always has an adiabatic crossing with the Rydberg–Rydberg states.

3.2. Example $5d_{5/2} + \hbar\omega \rightarrow 38p_{3/2}$

For contrast, in this section, we present results for a compact $d_{5/2}$ 'ground' state. All compact $d_{5/2}$ states present the same qualitative behavior. We chose the initial state to be the $5d_{5/2}$

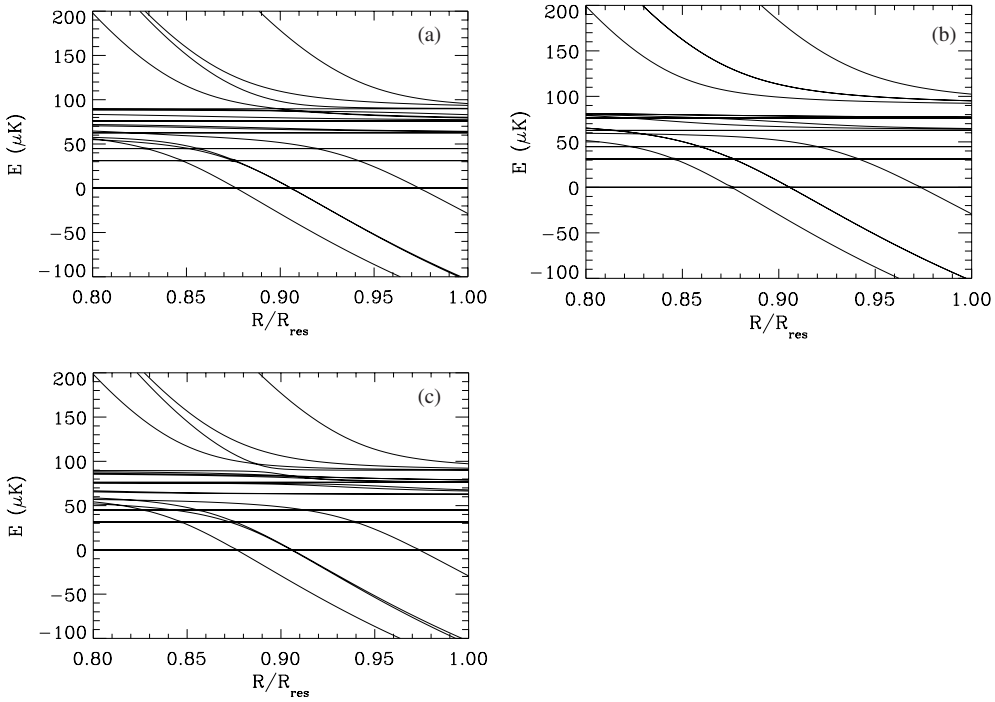

Figure 4. Same as figure 3 but for an expanded scale around the 2-photon avoided crossing.

state which gives a transition wavelength of $\sim$1.3 μm. We compute a radial dipole matrix element with the 38p state of 4×10^{-2} au by numerically solving for the radial functions in a model potential that gives the correct quantum defects. For the calculation, we chose the laser intensity to be 12 W cm^{-2}. Narrow linewidth diode sources at this frequency and intensity are available and relatively inexpensive.

First, we count the number of states: there are 36 states with $5d_{5/2}5d_{5/2}$ character, there are 24 states with $5d_{5/2}38p_{3/2}$ character and 24 with the order interchanged, there are 16 states with $38p_{3/2}38p_{3/2}$ character, and there are four states with $38s_{1/2}39s_{1/2}$ character and 4 with the order interchanged. This gives 108 states altogether.

In figure 3, we show the Floquet potential curves as a function of the atom separation for three different directions between the laser polarization and the interatomic direction. In all of the plots, the laser detuning was 5.50 MHz $\sim$ 264 μK. As in the previous section, there are several Rydberg–Rydberg potential curves and thus several resonance distances. Again, we define the scale length to be $R_{\rm res} \equiv (n^4/3\Delta)^{1/3}$ which corresponds to 5.0 μm for this case. Figure 4 shows a blowup of the region near the crossing of the ground state with the Rydberg–Rydberg state.

There are similar features between figures 2 and 3. The main qualitative difference arises from the degeneracy level of the ground state. There are 36 states with 5d5d character. There are only four Rydberg–Rydberg states that cross them. This means that only four of the ground states will adiabatically connect to the repelling potential curves. This can be seen clearly in figure 4. Furthermore, there are a large number of states that do not interact at all with the Rydberg–Rydberg states and these states have exact crossings. If a pair of atoms is in an initial state that does not adiabatically connect to the repelling potential curve, then the atoms will not feel a force. However, we note that the repelling potential curves are strongly coupled to

the ground states with the largest AC Stark shift. Hence, optical pumping might be used to ensure that primarily those states that adiabatically connect to the repelling Rydberg–Rydberg states are populated. Alternatively, one could use Rydberg states with a larger degeneracy factor (e.g. f-states) to increase the number of ground-Rydberg connections.

4. Discussion

The preceding sections provide only two of the many possible cases that might be explored. Clearly, the complexity of the control problem increases with the number of (nearly) degenerate orientations for the Rydberg–Rydberg and initial-state pairs. Nevertheless, the proposed method appears quite promising for real systems. The fraction of populated ground-state configurations which adiabatically connect to repulsive Rydberg–Rydberg curves is a key parameter for determining the effectiveness of any manipulation scheme based on this interatomic interaction. As noted above, this fraction can be enhanced by appropriate selection of laser polarization, focusing geometry, and perhaps external electric or magnetic fields.

5. Conclusion

We have proposed a method for manipulating the motion and position correlation function for cold atoms in a MOT. If successful the technique might be utilized to create an (approximately) ordered array of cold atoms without the need for confining optical lattice beams and/or to investigate long-range atomic scattering. The scheme exploits the separation sensitivity of the dipole–dipole interaction energy to enable excitation of ground-state atoms to repulsive Rydberg–Rydberg potential curves. The blue-detuned laser frequency determines the critical distance at which the atoms' approach is halted by the strong interatomic forces. Under appropriate conditions, the transfer of population into and out of the Rydberg states and the reflection of the atoms from each other can be accomplished with arbitrarily high efficiency. The atoms spend very little time in Rydberg states and remain cold and trapped within the MOT. Detailed calculations for the atomic dynamics within a reduced 5-state model are presented and complications associated with different degenerate ground- and final-state configurations are considered using two potential excitation schemes in Rb. The effectiveness of the method in the face of additional complications such as magnetic field inhomogeneity in the MOT (which would be difficult to accurately model) is being explored experimentally.

Acknowledgments

We are pleased to acknowledge stimulating discussions with T F Gallagher. This work was supported by the National Science Foundation under grant numbers 0355039 (MLW and FR) and 0355257 (RRJ).

References

[1] Raimond J M, Vitrant G and Haroche S 1981 *J. Phys. B: At. Mol. Phys.* **14** L655
[2] Singer K, Reetz-Lamour M, Amthor T, Fölling S, Tscherneck M and Weidemüller M 2005 *J. Phys. B: At. Mol. Opt. Phys.* **38** S321
[3] Reinhard A, Cubel Liebisch T, Knuffman B and Raithel G 2007 *Phys. Rev.* A **75** 032712
[4] Farooqi S M *et al* 2003 *Phys. Rev. Lett.* **91** 183002
[5] Jaksch D, Cirac J I, Zoller P, Rolston S L, Cote R and Lukin M 2000 *Phys. Rev. Lett.* **85** 2208
[6] Lukin M D, Fleischhauer M, Cote R, Duan L M, Jaksch D, Cirac J and Zoller P 2001 *Phys. Rev. Lett.* **87** 037901

[7] Tong D, Farooqi S, Stanojevic J, Krishnan S, Zhang Y, Cote R, Eyler E and Gould P 2004 *Phys. Rev. Lett.* **93** 063001
[8] Singer K, Reetz-Lamour M, Amthor T, Marcassa L and Weidemüller M 2004 *Phys. Rev. Lett.* **93** 163001
[9] Robicheaux F and Hernandez J V 2005 *Phys. Rev.* A **72** 063403
[10] Cubel Liebisch T, Reinhard A, Berman P R and Raithel G 2005 *Phys. Rev. Lett.* **95** 253002
[11] Vogt T, Viteau M, Zhao J, Chotia A, Comparat D and Pillet P 2006 *Phys. Rev. Lett.* **97** 083003
[12] Ates C, Pohl T, Pattard T and Rost J M 2006 *J. Phys. B: At. Mol. Opt. Phys.* **39** L233
[13] Hernandez J V and Robicheaux F 2006 *J. Phys. B: At. Mol. Opt. Phys.* **39** 4883
[14] Ates C, Pohl T, Pattard T and Rost J M 2007 *Phys. Rev. Lett.* **98** 023002
[15] Anderson W R, Veale J R and Gallagher T F 1998 *Phys. Rev. Lett.* **80** 249
[16] Mourachko I, Comparat D, de Tomasi F, Fioretti A, Nosbaum P, Akulin V and Pillet P 1998 *Phys. Rev. Lett.* **80** 253
[17] Frasier J S, Celli V and Blum T 1999 *Phys. Rev.* A **59** 4358
[18] Afrousheh K, Bohlouli-Zanjani P, Vagale D, Mugford A, Fedorov M and Martin J D D 2004 *Phys. Rev. Lett.* **93** 233001
[19] Robicheaux F, Hernandez J V, Topcu T and Noordam L D 2004 *Phys. Rev.* A **70** 042703
[20] Mudrich M, Zahzam N, Vogt T, Comparat D and Pillet P 2005 *Phys. Rev. Lett.* **95** 233002
[21] Afrousheh K, Bohlouli-Zanjani P, Carter J D, Mugford A and Martin J D D 2006 *Phys. Rev.* A **73** 063403
[22] Olson R E 1979 *Phys. Rev. Lett.* **43** 126
[23] Safinya K, Delpech J, Gounand F, Sandner W and Gallagher T 1981 *Phys. Rev. Lett.* **47** 405
[24] Gallagher T F 1994 *Rydberg Atoms* (Cambridge: Cambridge University Press) and references therein
[25] Walz-Flannigan A, Guest J R, Choi J-H and Raithel G 2004 *Phys. Rev.* A **69** 063405
[26] Carroll T J, Claringbould K, Goodsell A, Lim M J and Noel M W 2004 *Phys. Rev. Lett.* **93** 153001
[27] Robicheaux F 2005 *J. Phys. B: At. Mol. Opt. Phys.* **38** S333
[28] Knuffman B and Raithel G 2006 *Phys. Rev.* A **73** 020704
[29] Tan J N, Bollinger J J, Jelenkovic B and Wineland D J 1995 *Phys. Rev. Lett.* **75** 4198
[30] Berkeland D J, Miller J D, Bergquist J C, Itano W M and Wineland D J 1998 *Phys. Rev. Lett.* **80** 2089
[31] Vala J, Thapliyal A V, Myrgren S, Vazirani U, Weiss D S and Whaley K B 2005 *Phys. Rev.* A **71** 032324
[32] Boisseau C, Simbotin I and Cote R 2002 *Phys. Rev. Lett.* **88** 133004
[33] de Oliveira A L, Mancini M W, Bagnato V S and Marcassa L G 2003 *Phys. Rev. Lett.* **90** 143002
[34] Walker T G and Saffman M 2005 *J. Phys. B: At. Mol. Opt. Phys.* **38** S309
[35] Marcassa L G, de Oliveira A L, Weidemüller M and Bagnato V S 2005 *Phys. Rev.* A **71** 054701
[36] Schwettmann A, Crawford J, Overstreet K R and Shaffer J P 2006 *Phys. Rev.* A **74** 020701(R)
[37] Amthor T, Reetz-Lamour M, Westermann S, Denskat J and Weidemüller M 2007 *Phys. Rev. Lett.* **98** 023004
[38] Marcassa L, Muniz S, de Queiroz E, Zilio S, Bagnato V, Weiner J, Julienne P S and Suominen K-A 1994 *Phys. Rev. Lett.* **73** 1911
[39] Gensemer S D and Gould P L 1998 *Phys. Rev. Lett.* **80** 936
[40] Wright M, Gensemer S, Vala J, Kosloff R and Gould P 2005 *Phys. Rev. Lett.* **95** 063001
[41] Wright M J, Pechkis J A, Carini J L and Gould P L 2006 *Phys. Rev.* A **74** 063402
[42] Fioretti A, Comparat D, Drag C, Gallagher T F and Pillet P 1999 *Phys. Rev. Lett.* **82** 1839
[43] Li W, Tanner P J and Gallagher T F 2005 *Phys. Rev. Lett.* **94** 173001
[44] Li W, Mourachko I, Noel M W and Gallagher T F 2003 *Phys. Rev.* A **67** 052502
[45] Edmonds A R 1974 *Angular Momentum in Quantum Mechanics* 2nd edn (Princeton, NJ: Princeton University Press)